Chiral Nonlocal Metasurfaces for Frequency-Selective Wavefront Shaping

Yoshiaki Kasahara⁽¹⁾, Adam Overvig ⁽²⁾, and Andrea Alù^(1, 2)

- (1) The University of Texas at Austin, Austin, Texas, 78712, USA (ykasahara@utexas.edu)
 - (2) City University of New York, New York, 10031, USA (aalu@gc.cuny.edu)

Abstract—We propose, design, and experimentally demonstrate a nonlocal metasurface with frequency-selective, wavefront shaping capabilities and at the same time polarization-selective chiral response. This operation requires the implementation of bilayer metasurfaces with engineered nonlocal response, wherein each layer controls locally a specific linear polarization, while the coupled system supports arbitrary polarization states. We demonstrate that this platform enables unprecedented control over wavefront manipulation, including frequency-selective, spin-selective reflection with arbitrary geometric phase. We observe a highly chiral response with record-high reflectance efficiency over a narrow frequency window, both for a uniform metasurface and for one with tailored phase gradient for anomalous reflection. Both devices provide an efficiency well above the theoretical limit of 25% for conventional single-layer devices. Our work opens exciting opportunities for augmented reality and enhanced secure wireless communications.

I. INTRODUCTION

Metasurface (MS) technology has been spearheading exciting opportunities for electromagnetics and optics. MSs can be classified into distinct two groups, with local and nonlocal responses, respectively [1-5]. While a local MS locally resonates and spatially controls the amplitude and phase of the impinging wave at each location [1], a nonlocal MS supports spatially extended resonances, and therefore it is effective to control the impinging frequency spectrum [2-5]. This spectral selectivity can be controlled by the degree of perturbation in structures with high symmetry [3]. Although nonlocal MSs conventionally are not able to shape the reflected or transmitted wavefronts, in [4] a phase gradient nonlocal MS has been recently shown to enable both wavefront control and spectral selectivity. The efficiency of such operation is fundamentally limited to 25% in singlelayer MSs, due to out-of-plane symmetry [2-4]. Bi-layer MSs can overcome this limit, and selectively shape the wavefront with 100% efficiency for arbitrary polarization [5]. In this work, we demonstrate for the first time such operation, showing nonlocal MSs that support efficient, arbitrarily chiral, polarizationselective, and frequency-selective manipulation of the input wavefront. We optimized, fabricated and measured two devices: the first with a uniform profile consisting of identical unit cells, verifying chiral selectivity with high efficiency and the second one with a phase gradient that also enables wavefront shaping.

II. UNIT CELL AND METASURFACE DESIGN

Our nonlocal chiral MS consists of planar metallic ellipses, in contrast to volumetric structures used in the optical regime [2-5]. The ellipse eccentricity determines the degree of perturbation from a circular shape that enables coupling from free space to a

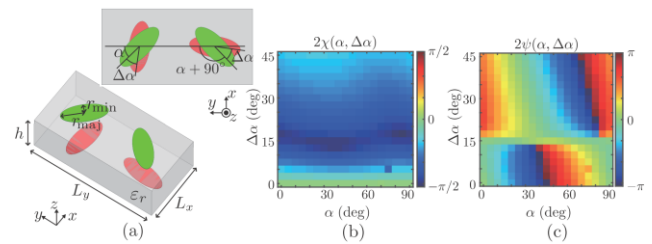


Figure 1. (a) Unit cell of nonlocal MSs. The four metallic ellipses are identical with their major radius, $r_{\rm maj} \sim 1.93$ mm (this parameter is slightly tuned for the gradient MS design), and minor radius $r_{\rm min} \sim 0.47$ mm. Other parameters are $L_x = 5.2$ mm, $L_y = 2L_x$, h = 3.2 mm, and $\varepsilon_r = 2.55$, assuming a substrate AD255C. (b) Latitude and longitude on the Poincaré sphere for eigen-polarizations of the unit cell as we vary α and $\Delta\alpha$.

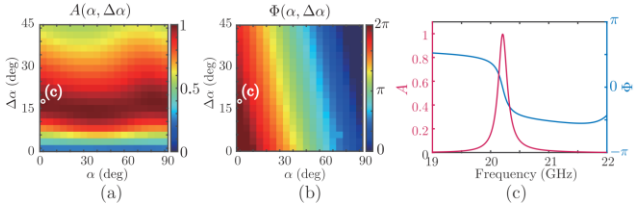


Figure 2. (a) Amplitude and (b) phase of the reflected wave for RHCP illumination. (c) Frequency response of the unit cell with $\alpha = 0^{\circ}$ and $\Delta \alpha = 17.5^{\circ}$, marked by a white circle in Fig. 2(a) and (b).

leaky wave supported by the MS. Bilayer structures can introduce chirality in their response when each layer scatters an orthogonal linear polarization; a geometric phase is obtained based on the orientation angles of these linear polarizations. A polarization state, resonating with the MS and therefore leading to unitary reflection in the absence of loss, is the eigen-polarization state [4-5]. In our chiral nonlocal MS, the eigen-polarization may be arbitrarily tuned around the entire Poincaré sphere by varying the angles α and $\Delta\alpha$ in Fig. 1(a). For each pair of α and $\Delta\alpha$, we show the corresponding eigen-polarization in Figs. 1(b) and (c), calculated with full-wave simulations for a periodic MS. The eigen-polarization moves over the Poincaré sphere latitudinally (2γ) with a change of $\Delta\alpha$, and longitudinally (2Ψ) with a change of α , in agreement with the idealized relations in [5]: $\Psi\sim 2\alpha+\Delta\alpha$ and $\chi\sim \Delta\alpha$.

The response of such an ideal nonlocal MS for right-handed circular polarization (RHCP) is $E_R = [1+\sin(2\chi)]e^{-2\gamma\Psi}/2$, which shows that the amplitude (A) and phase (Φ) of the reflected wave are controlled by χ and Ψ . These properties are confirmed in Fig. 2 (a,b): unitary reflection is found around $\Delta\alpha \sim 17.5^{\circ}$ for any value of α in Fig. 2(a), and the phase of the reflected wave can vary over 2π by changing α in Fig. 2(b). Thus, by synthesizing the MS unit cells with properly selected α and $\Delta\alpha$, we can build a chiral nonlocal MS with arbitrary profile of geometric phase.

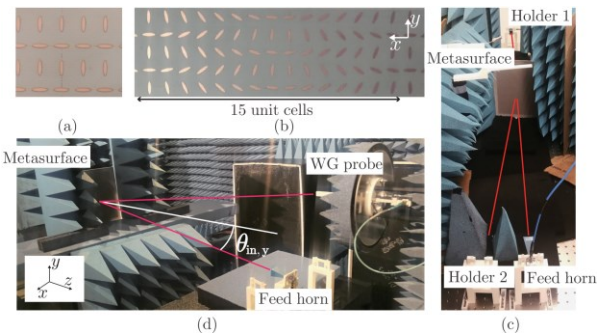


Figure 3. Photos of fabricated (a) uniform MS and (b) phase-gradient MS. (c) Experimental setup to evaluate transmission and reflection efficiencies. (d) Setup to measure anomalous reflection.

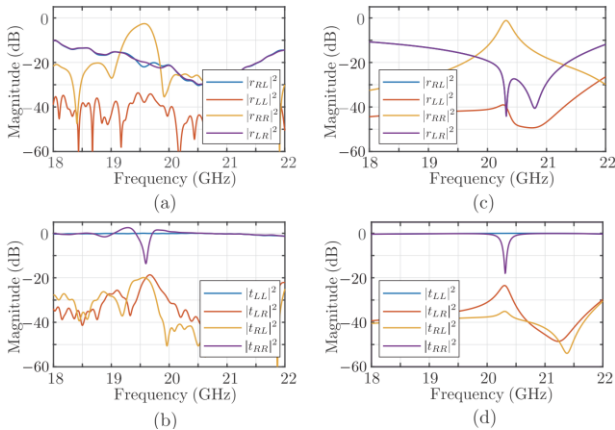


Figure 4. S-parameters of the uniform MS in the circular-polarization basis. Measured (a) reflection and (b) transmission. Simulated (c) reflection and (d) transmission.

The frequency-selective response of the unit cell with $\alpha = 0^{\circ}$ and $\Delta \alpha = 17.5^{\circ}$ is shown in Fig. 2(c). Its spectral linewidth can be controlled by altering the perturbation magnitude and is confirmed in our design [3].

III. METASURFACE CHARACTERIZATION

Photos of our two fabricated MSs are shown in Fig. 3(a,b). The first is a uniform MS with $\alpha = 0^{\circ}$ and $\Delta \alpha = 17.5^{\circ}$, selectively reflecting RHCP illumination over a narrow bandwidth. The second MS has a linear phase gradient, realized varying α from 0° to 180° in the x-direction, with $\Delta \alpha \sim 72.5^{\circ} (= 90^{\circ} - 17.5)$ to maximize efficiency for circular polarization selectivity. The encoded phase changes over a 4π range rather than 2π [see Fig. 2(b)]. One period consists of 15 unit cells, and it is expected to add a transverse momentum $k_x = -0.41k_0$ to the impinging wave.

We characterize transmission and reflection using the setup in Fig. 3(c). The receiver antenna is placed on holder 1 for transmission and on holder 2 for reflection measurements. The *S*-parameters for circular polarization are constructed from the measurement results of every pair of linear polarizations. They are normalized using calibration measurements without MS for transmission and with a metallic plate of same size for reflection. The uniform MS shows a reflection efficiency of 55% (-2.6 dB) for RHCP signals ($|r_{RR}|^2$) [Fig. 4(a)], exceeding the 25% limit of conventional MSs [2-4]. The corresponding transmission for RHCP ($|t_{RR}|^2$) in Fig. 4(b) drops to 4.0% (-14 dB), showing perfect chirality. The opposite circular polarization does not engage

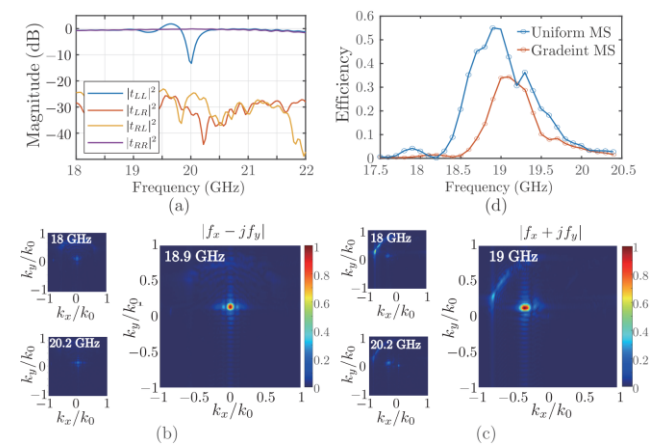


Figure 5. (a) Transmission S-parameter of gradient MS. Fourier spectrum for (b) uniform MS and (c) phase-gradient MS. (d) Estimated efficiencies.

at all the MS, which remains transparent, in agreement with the simulation in Fig.4 (c,d). The lower *Q*-factor around 58 in experiments versus 110 in simulations, together with the non-ideal efficiency, can be attributed to the non-plane wave excitation and the finite size of the MS. We performed the same measurements for the phase-gradient MS in transmission, shown in Fig. 5(a), demonstrating excellent chiral polarization-selective and frequency-selective response as well: the extinction for transmitted left-handed wave is 6.2% (-12 dB) on resonance.

The anomalous reflection of the phase-gradient MS is measured with the setup in Fig. 3(d). The reflected waves from the horn antenna are captured by a position-scanning waveguide (WG) probe. While the uniform MS shows a peak of normalized reflected wave at the transverse momentum $(k_x, k_y) = (0, 0.13)k_0$ in Fig. 5(b), where the shift in k_y is due to the finite incident angle of $\theta_{\text{in},y}$ = 10°, the gradient MS shows its peak at (k_x, k_y) = (0.40, $(0.13)k_0$ in Fig. 5(c), as expected by the encoded phase gradient. These peaks disappear off resonance [insets in Fig. 5(b,c)] and for opposite polarization. The estimated efficiencies in Fig. 5(d) show that the phase gradient anomalously reflects the incident beam to the -2 diffractive order with an efficiency of 34%. The shift of resonant frequencies between Figs. 5(a) and (d) can be predicted through the dispersion with the incident angle $\theta_{in,y}$. In summary, our fabricated nonlocal MSs demonstrates unprecedented frequency-selective, polarization-selective, efficient wavefront manipulation, ideally suited for wireless communication systems. Translated to the optical domain, this response can enable exciting opportunities for augmented reality.

REFERENCES

- C. Pfeiffer, and A. Grbic, "Bianisotropic metasurface for optical polarization control: analysis and synthesis," *Phys. Rev. Appl.*, vol. 2, pp. 044011, Oct. 2014.
- [2] A. Tittl, A. Leitis, M. Liu, F. Yesilkoy, D. Y. Choi, D. N. Neshev, S. Yuri, and H. Altug, "Imaging-based molecular barcoding with pixelated dielectric metasurfaces," *Science*, vol. 360, pp.1105-1109, Jun. 2018.
- [3] K. Koshelev, S. Lepeshov, M. Liu, A. Bogdanov, and Y. Kivshar, "Asymmetric metasurfaces with high-Q resonances governed by bound states in the continuum," *Phy. Rev. Lett.*, vol. 121, 193903, Nov. 2018.
- [4] S. C. Malek, A. Overvig, S. Shrestha, and N.Yu, "Resonant wavefront-shaping metasurfaces based on quasi-bound states in the continuum" in Conference on Lasers and Electro-Optics (CLEO), pp. 1-2, May 2020.
- [5] A. C. Overvig, N. Yu, and A. Alù, "Chiral quasi-bound states in the continuum," *Phys. Rev. Lett.*, vol. 126, pp.073001, Feb. 2021.